



Magnetic Resonance Imaging for Liver Cirrhosis

Sarah Al Sayed Mahmoud Metwally, Ayman Fathy Zeid, Hamed Abdel Hakim Gobran, Mostafa Mohamad Assy

Radiodiagnosis Department, Zagazig University Hospital, Egypt

Corresponding Author: Sarah Al Sayed Mahmoud Metwally

Email: sarahalsayed710@yahoo.com

Abstract

Background: Cirrhosis is impaired liver function caused by formation of scar tissue known as fibrosis, due to damage caused by liver disease. Damage causes tissue repair and subsequent formation of scar tissue, which over time can replace normal functioning tissue leading to cirrhosis and impaired liver function. Early symptoms may include tiredness, weakness, loss of appetite, unexplained weight loss, nausea and vomiting, and discomfort in the right upper quadrant of the abdomen. Important criteria for determining the presence of cirrhosis in the clinical setting include (a) morphologic features of the liver (based on the atrophy or hypertrophy of various liver segments), (b) liver contours (irregular contour), (c) presence of nodules within the liver parenchyma, (d) the signal intensity of the liver as well as of the nodules, (e) the presence of fatty infiltration or iron, and (f) the presence of vascular and biliary tree abnormalities. In evaluating liver lesions at imaging, the single most important step consists of evaluating the background liver for the presence of diffuse disease and determining the presence of cirrhosis. In the absence of cirrhosis, the differential diagnosis of a hypervascular liver lesion in particular is relatively extensive and may include benign liver lesions such as arterioportal shunts, flash-filling hemangiomas, hepatocellular adenomas, and FNH, and malignant liver lesions including hypervascular metastases and HCCs.

Keywords: Magnetic Resonance Imaging, Liver Cirrhosis

DOI Number: 10.14704/nq.2022.20.8.NQ44280

NeuroQuantology 2022; 20(8): 2602: 2608

Introduction

Cirrhosis is impaired liver function caused by formation of scar tissue known as fibrosis, due to damage caused by liver disease. Damage causes tissue repair and subsequent formation of scar tissue, which over time can replace normal functioning tissue leading to cirrhosis and impaired liver function (1).

Early symptoms may include tiredness, weakness, loss of appetite, unexplained weight loss, nausea and vomiting, and discomfort in the right upper quadrant of the abdomen (2).

As the disease worsens, symptoms may include itching, lower limb edema, ascites, jaundice (2).

Cirrhosis affected about 2.8 million people and resulted in 1.3 million deaths in 2015. Of these deaths, alcohol caused 348,000, hepatitis C caused 326,000, and hepatitis B caused 371,000.

Signs and symptoms:

I. Liver dysfunction

These features are a direct consequence of liver cells not functioning:

- Spider angiomas or spider nevi are vascular lesions consisting of a central arteriole surrounded by many smaller vessels and occur due to an increase in estradiol. Spider angiomas occur in about one-third of cases (3).



- Palmar erythema is a reddening of palms at the thenar and hypothenar eminences seen in about 23% of cirrhosis cases as a result of increased estrogen (4).
- Gynecomastia, or benign increase in breast size in men, is caused by increased estradiol and can occur in up to two-thirds of cases (5).
- Hypogonadism, a decrease in male sex hormones, may manifest as impotence, infertility and loss of sexual desire.
- Liver size can be enlarged, normal, or shrunken in people with cirrhosis.
- Ascites.
- Jaundice, yellow discoloration of the skin and mucous membranes, due to increased bilirubin level, which may also cause the urine to be dark colored (6).

II. Portal hypertension

Liver cirrhosis increases resistance to blood flow and leads to higher pressure in the portal venous system, resulting in portal hypertension. Effects of portal hypertension include:

- Splenomegaly; found in 35 to 50% of cases (7).
- Esophageal varices result from collateral portal blood flow through vessels in the stomach and esophagus (porto-caval anastomosis or shunting).
- Caput medusea; dilated paraumbilical collateral veins due to portal hypertension (6).

III. Other nonspecific signs

Some signs that may be present but not specific include changes in the nails (such as Muehrcke's lines, Terry's nails, and nail clubbing), hypertrophic osteoarthropathy, and Dupuytren's contracture (8).

IV. Advanced disease

As the disease progresses, complications may develop. In some people, these may be the first signs of the disease.

- Bruising and bleeding can result from decreased production of clotting factors.
- Hepatic encephalopathy (HE) occurs when ammonia and related substances build up in the blood and affect brain function when they are not cleared from the blood by the liver. This may result in neglect of personal appearance, unresponsiveness, forgetfulness, trouble concentrating, changes in sleep habits, or psychosis. One classic physical examination finding is flapping tremors. Feter hepaticus is a musty breath odor resulting from increased dimethyl sulfide and is a feature of HE (9).
- Acute kidney injury (particularly hepatorenal syndrome)
- Cachexia associated with muscle wasting and weakness (10)

An understanding of the segmental hepatic anatomy by magnetic resonance imaging with recognition of the major hepatic landmarks and vascular structures is essential for correct pre-operative localization of hepatic masses. Moreover, it enables the radiologist to take axial, sagittal and coronal images when evaluating the liver (11).

➤ Axial images:

The normal liver parenchyma appears homogenous on both T1 and T2 weighted images. The liver shows isointense signal on T1 weighted images. The liver has a signal intensity similar to that of the pancreas but brighter than the spleen or the kidneys. On T2 weighted images, the liver appears darker and has signal intensity similar to that of muscle and significantly less than that of the kidneys and spleen (11).

The major vascular structures are most consistently demonstrated in the axial MR images. With spin echo MRI, generally vessels are delineated as areas of signal void **(12)**

The inferior vena cava is consistently demonstrated as a round, signal void structure grooving the postero-inferior surface of the liver between the right and caudate lobes **(13)**.

Hepatic veins are intersegmental and drain parts of adjacent segments. Left hepatic vein separates segment II from IV. Middle hepatic vein separates segment IV from segments V and VIII. Right hepatic vein separates anteriorly situated segments V and VIII from posteriorly situated segments VI and VII **(12)**.

The course of the portal vein usually seen on axial images as it passes from its retro-pancreatic location, through the hepato duodenal ligament, and into the porta hepatis. Oblique coronal MRI images can demonstrate the entire length of the main portal vein **(13)**.

The right portal vein has an anterior branch that lies centrally within the anterior segment of the right lobe and posterior branch that lies centrally within the posterior segment of the right lobe. The portal vein divides into the sectorial and the segmental branches very close to the hepatic hilum, in each sector the inferior segments (V and VI) will be caudal to portal bifurcation, and the superior segments (VII and VIII) will be cranial to it. Therefore, the right anterior sector segment V will be below and segment VIII above, and in the posterior sector segment VI below and segment VII above. Left portal vein divides left lobe in superior segments (IVa & II) and inferior segments (IVb & III) **(12)**.

Liver MR Imaging Technique:

A typical liver MR imaging protocol (at 1.5 T) should contain the following or similar types of sequences (Table 1).

*Performed with fat suppression before and after the injection of gadolinium-based contrast material during the arterial phase and several other phases.

†Non-breath-hold, respiratory-triggered sequence performed with fat suppression.

1. Coronal single-shot turbo or fast spin-echo sequence (single breath hold): serves as a localizer and provides an overview of the anatomy.
2. Axial single-shot turbo spin-echo sequence with a relatively longer echo time helps distinguish between fluid-filled and solid liver lesions. This sequence is heavily T2 weighted and is often used in combination with other moderately T2-weighted sequences.
3. Axial two-dimensional dual GRE sequence (both in-phase and opposed-phase imaging during a single breath hold): provides T1 information and helps detect focal or diffuse fatty infiltration in tumors and tissues.
4. Axial dynamic 3D fat-suppressed GRE sequence (vendor-specific acronyms: performed during all phases for the detection and characterization of lesions on the basis of their enhancement patterns. Arterial phase imaging is performed with bolus tracking and is the single most important sequence for the detection of liver lesions. Some institutions perform a multiarterial phase sequence as an alternative to single-phase imaging to further improve the detection of hypervascular liver lesions **(14)**).

5. Coronal or axial 3D delayed phase fat-suppressed GRE sequence (performed after axial contrast-enhanced imaging, about 5 minutes after injection; section thickness, 4–6 mm, interpolated to about 40 overlapping reconstructed sections of 2–3 mm each): provides information about the persistent enhancement of lesions such as hemangiomas, the washout and capsular enhancement of HCC, peritoneal spread of disease, and biliary tree abnormalities.
6. Axial fat-saturated turbo or fast spin-echo T2-weighted sequence (2–3 signals acquired): has traditionally been used for the detection of solid liver lesions, lymph nodes, and edema. Most likely, it will be replaced by newer T2-weighted sequences such as black-blood echoplanar imaging.
7. Axial black-blood echoplanar T2-weighted imaging (frequency and phase matrix, 144 × 256; field of view, 310–350 cm with a rectangular field of view of 80%; echoplanar imaging factor, 109; sensitivity-encoding factor, 2; half-scan factor, 60%; *b* value, 20; bandwidth per pixel in the phase-encoding direction, 9.2 Hz, and in the echoplanar imaging readout direction, 1387.1 Hz; polarity of the phase-encoding gradient, posterior): provides breath-hold T2-weighted images with better liver-to-lesion contrast than can be achieved with standard fat-suppressed turbo spin-echo T2-weighted imaging. This pulse sequence is an alternative to the standard T2-weighted sequence (15)

Table (1): Commonly used sequences and parameters in liver MRI imaging (15)

Sequence	Parameter				Function	Remarks
	TR (msec)	TE (msec)	Flip angle (°)	Acquisition time (sec)		
Coronal SSTSE	∞	120	90	20	Localization; overview of anatomy	Alternative sequences: balanced steady-state (FIESTA, balanced FFE, True FISP)
Axial SSTSE	∞	180	90	20	Detection of fluid-filled lesions, distinction between fluid-filled and solid lesions	Combine with moderately T2-weighted sequences such as respiratory-triggered T2-weighted FSE, STIR-FSE, and BBPEI
2D dual GRE	150–170	2.1/4.2	80–90	20	T1 information and fat detection	Modified Dixon-based 3D techniques are likely to replace dual GRE
3D GRE*	Minimum	Minimum	10–15	20–25	Detection and characterization of lesions on the basis of enhancement patterns	Multiarterial phase sequence is an alternative (20)
Delayed phase 3D GRE	Minimum	Minimum	10–15	20–25	Enhancement patterns of lesions	...
T2-weighted FSE or TSE†	2000	80–100	90	120–300	Detection of solid liver lesions	Alternatives: STIR-FSE and BBPEI
BBPEI	3400	60	...	25	Detection of solid liver lesions	Alternatives: STIR-FSE and T2-weighted FSE

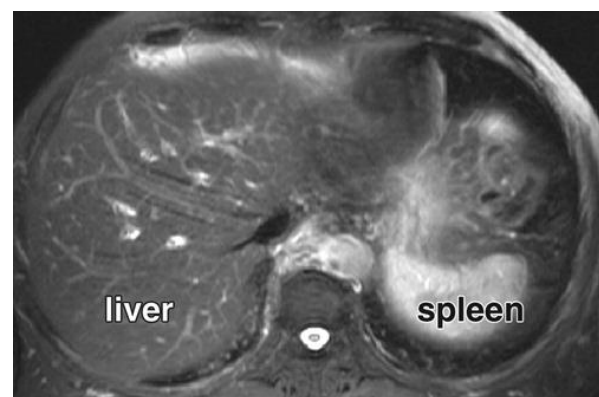


Fig (1): Typical MR imaging examination of the liver. (a) On an axial standard fat-suppressed T2-weighted MR image, the spleen is much brighter than the liver. This sequence is considered to be sensitive for the depiction of solid liver lesions, which typically follow the signal intensity of the spleen. (16)



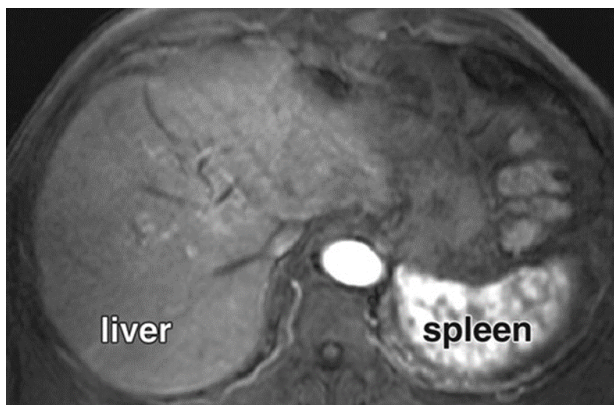


Figure (2) Axial 3D arterial phase GRE T1-weighted image obtained with bolus tracking shows no pathologic findings. This sequence is the single most important sequence for the detection and characterization of focal liver lesions. (16)

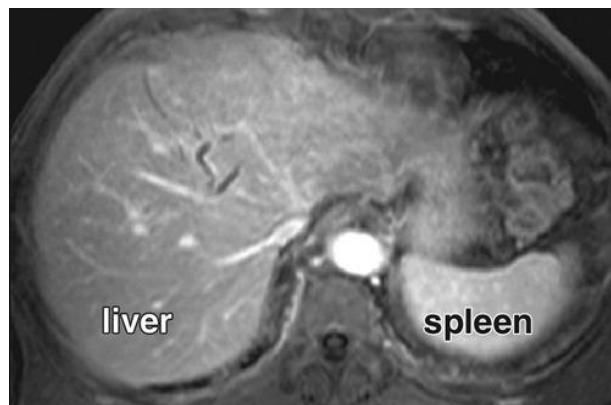


Figure (4) Axial 3D delayed phase GRE T1-weighted image obtained 2–5 minutes after contrast material injection shows no pathologic findings. This sequence is essential for the further characterization of liver lesions detected during the arterial phase. (16)

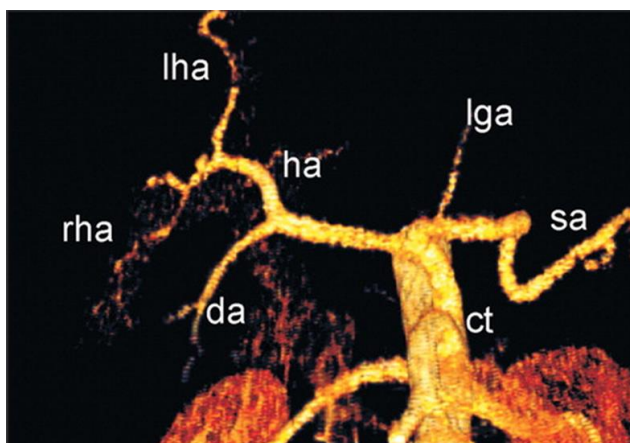


Figure (3): Volume-rendered image from dynamic gadolinium-enhanced arterial phase imaging data obtained in a different patient shows the celiac trunk (*ct*), duodenal artery (*da*), hepatic artery (*ha*), left gastric artery (*lga*), left hepatic artery (*lha*), right hepatic artery (*rha*), and splenic artery (*sa*). (17)

Determining the Presence of Cirrhosis with MR Imaging:

Important criteria for determining the presence of cirrhosis in the clinical setting include (a) morphologic features of the liver (based on the atrophy or hypertrophy of various liver segments), (b) liver contours (irregular contour), (c) presence of nodules within the liver parenchyma, (d) the signal intensity of the liver as well as of the nodules, (e) the presence of fatty infiltration or iron, and (f) the presence of vascular and biliary tree abnormalities (15).

Evaluating Lesions in Cirrhotic Livers with MR Imaging:

In evaluating liver lesions at imaging, the single most important step consists of evaluating the background liver for the presence of diffuse disease and determining the presence of cirrhosis.

In the absence of cirrhosis, the differential diagnosis of a hypervascular liver lesion in particular is relatively extensive and may include benign liver lesions such as arterioportal shunts, flash-filling hemangiomas, hepatocellular adenomas, and FNH, and malignant liver lesions including hypervascular metastases and HCCs (15).

If cirrhosis is present, the differential diagnosis of a hypervascular liver lesion can be narrowed to a few entities, including arterioportal shunts or pseudolesions (for very small lesions), dysplastic nodules, and HCCs. Occasionally, a cirrhotic liver may have preexisting flash-filling hemangiomas that may mimic malignant lesions. By definition, hepatocellular adenoma and FNH should not be diagnosed within a cirrhotic liver (18). Hyperplastic nodules similar to FNH may occur in cirrhotic livers but distinguishing them from HCC at imaging is difficult (19).

References

1. **Dooley, James (James S.),, Lok, Anna S. F.,, Garcia-Tsao, Guadalupe,, Pinzani, Massimo.** Sherlock's diseases of the liver and biliary system (Thirteenth ed.). Hoboken, NJ. 2018. p. 82. ISBN 978-1-119-23756-3. OCLC 1019837000. Archived from the original on 30 July 2021. Retrieved 7 December 2020.
2. **National Institute of Diabetes and Digestive and Kidney Diseases. 2021;** "Symptoms & Causes of Cirrhosis | NIDDK". Retrieved 8 February 2021.
3. **Li CP, Lee FY, Hwang SJ, et al.** Spider angiomas in patients with liver cirrhosis: role of alcoholism and impaired liver function. **Scand. J. Gastroenterol.**1999; 34 (5): 520–3.
4. **William, James.** Andrews' Diseases of the Skin: Clinical Dermatology. **Saunders.**2005; ISBN 978-0-7216-2921-6.
5. **Slater, Joseph S. Esherick, Daniel S. Clark, Evan D.** Current practice guidelines in primary care 2013. New York: **McGraw-Hill Medical.**2012; pp. Chapter 3: Disease Management.
6. **Longo, Dan L.; et al.,** Harrison's principles of internal medicine (18th ed.). New York: **McGraw-Hill.** pp.2012; Chapter 308. Cirrhosis and Its Complications. .
7. **Friedman LS** (2014). Current medical diagnosis and treatment 2014. [S.l.]: Mcgraw-Hill. pp. Chapter 16. Liver, Biliary Tract, & Pancreas Disorders.
8. **uurmond, D.** *Color Atlas and Synopsis of Clinical Dermatology: Common and Serious Diseases.* **McGraw-Hill.** pp. Section 33: *Disorders of the nail apparatus.*2009;
9. **Tangerman, A; Meuwese-Arends, MT; Jansen, JB.** Cause and composition of foetor hepaticus. **Lancet.**1994; 343 (8895): 483.
10. **Plauth, Mathias; Schütz, Elke-Tatjana.** Cachexia in liver cirrhosis. **International Journal of Cardiology.**2002; 85 (1): 83–87.
11. **Reimer P, Parizel P, Tombach B, et al., (2006):** Liver and biliarysystem. By Reimer and Stichenton (eds) in clinical MR imaging: A practical approach. 2nd edition, Schering,Germany. Springer Berlin Heidelberg New York; (9): PP: 272-318.
12. **Robinson P and Ward J. (2006):** MRI of the Liver. Robinson and Ward (eds). MRI of the Liver; a Practical Guide. By Taylor and Francis Group, New York. Part A, ch (4): 67-73.
13. **Nitz W. (2002):** Fast and ultrafast non echo planar MR Imaging techniques. *Eur Rad*; 12:2866-2882.
14. **Ito K, Fujita T, Shimizu A et al.,** Multiarterial phase dynamic MRI of small early enhancing hepatic lesions in cirrhosis or chronic hepatitis: differentiating between hypervascular hepatocellular carcinomas and pseudolesions. **AJR Am J Roentgenol** 2004 ;183: 699–705.
15. **Hussain SM, De Becker J, Hop WC, Dwarkasing S, Wielopolski PA.** Can a single-shot black-blood T2-weighted spin-echo echo-planar imaging sequence with sensitivity encoding replace the respiratory-triggered turbo spin-echo sequence for the liver? an optimization and feasibility study. **J Magn Reason Imaging** 2005; 21:219–229.



16. **Coenegrachts K.** Magnetic resonance imaging of the liver: new imaging strategies for evaluating focal liver lesions. **World J Radiol.** 2009 Dec 31;1(1):72-85.
17. **Gündoğdu, Elif & Kebapçı, Mahmut. (2021).** Two novel hepatic arterial variations in a living liver donor detected by multidetector computed tomography angiography. **Surgical and Radiologic Anatomy.** 43.
18. **International Working Party.** Terminology of nodular hepatocellular lesions. **Hepatology** 1995; 22:983–993.
19. **van den Bos IC, Hussain SM, Terkivatan T, Zondervan PE, de Man RA.** Stepwise carcinogenesis of hepatocellular carcinoma in the cirrhotic liver: demonstration on serial MR imaging. **J Magn Reson Imaging** 2006; 24:1071–1080.